Surface finish effect on dry sliding wear behavior of thermally oxidized commercially pure zirconium

A. Alansari, Y. Sun*

School of Engineering and Sustainable Development
Faculty of Technology
De Montfort University
Leicester, UK

* Corresponding author: ysun01@dmu.ac.uk

Abstract

The aim of this work was to investigate the effect of surface polishing on the wear behavior of thermally oxidized commercial pure zirconium (CP-Zr) under dry sliding conditions. Surface ground CP-Zr with a roughness of 0.21 μm (R_a) was thermally oxidized (TO) at 650 °C for 6 h. After TO, some samples were polished to smoothen the surface with a finish of 0.04 μm (R_a). The response of the polished and unpolished TO samples to dry sliding wear was investigated under unidirectional sliding conditions. The results show that surface polishing after TO affects the dry sliding wear behavior of TO CP-Zr in several aspects, including coefficient of friction, wear rate, crack formation and oxide layer breakdown. In particular, it is found that smoothening the TO surface favors the formation of semi-circular cracks in the wear track and accelerates oxide layer breakdown during dry sliding. A slightly rough TO surface helps to reduce the tendency of the oxide layer towards cracking and to increase the wear resistance at high contact loads. The mechanisms involved are discussed in terms of asperity contacts, crack formation, propagation and final fracture.

Keywords: zirconium, thermal oxidation, zirconium oxide, surface finish, friction, wear

1. Introduction

Zirconium and its alloys are technologically important materials which possess adequate mechanical strength, excellent corrosion resistance, good biocompatibility and neutron transparency [1,2]. They have found increasing applications in various sectors of industry, for example to make artificial implants in the biomedical industry [2,3], to make pressure tubes and fuel channels for nuclear power generation [1] and to make chemical processing equipment [4]. However, Zr has low hardness (about 200 HV) and a HCP crystal structure with a c/a ratio of 1.593, which deviates from the ideal value of 1.633. Thus, zirconium has inadequate tribological properties and suffers from severe metallic wear during sliding contact motions [5,6]. Without appropriate surface modification, Zr and its alloys are not suitable for tribological applications.

Thermal oxidation [5-8] and plasma electrolytic oxidation [9,10] are currently the most widely used techniques to enhance the surface hardness and wear resistance of Zr and its alloys. In particular, thermal oxidation is a simple process carried out in air furnaces at 550 °C to 800 °C

to produce a relatively thick (a few microns) zirconium oxide (ZrO_2) layer at the surface and an oxygen diffusion zone (ODZ) at the subsurface [8,11]. Thermally oxidized zirconium possesses a ceramic ZrO_2 layer for wear resistance, a hardened subsurface to bear the load and a tough core to provide fracture resistance [6,8].

Thermally oxidized zirconium (TO-Zr), as an alternative to the most commonly used Co-Cr alloys, has been used in artificial hip and knee joints [12-14]. One of the benefits of oxidized Zr in arthroplasty is its extremely good resistance to surface scratching which may be caused by trapped hard particles [14-17], which is crucial for reducing wear of the counter articulating part made of polyethylene (PE). In such an application, a very smooth and polished TO surface is necessary. However, TO-Zr also has potential uses in other fields involving sliding contact motions [5], where a polished surface may not be necessary. In manufacturing engineering components, smoothening by polishing is quite time consuming and costly. Therefore, polishing operations should be avoided whenever possible [18].

Surface finish is known to affect the tribological performance of engineering components and the counter bodies [19,20]. The friction and wear properties could be affected by surface roughness by altering the contact conditions, the stress distribution, the ploughing actions and the adhesion behaviour [21-23]. The majority of published investigations have found that a rougher surface results in a higher wear rate from both the component and the counter body [24,25]. When frictional behaviour is concerned, the effect of surface roughness is more complicated, because friction is affected by many factors, such as the adhesion junctions formed at the real contact areas, the ploughing actions of the asperities, the trapped wear particles and the mechanical interlocking of asperities. Depending on sliding contact conditions and contacting materials involved, rougher surfaces may result in higher friction [18,22,26,27] or lower friction [21,25], or have no effect on friction [23]. Most of the investigations concerning surface roughness effect on tribology have been focused on friction and wear rate, very few work have been reported on the effect of surface finish on the formation of cracks and their propagation in coating systems during dry sliding wear.

In the present work, surface ground commercially pure zirconium (CP-Zr) with a surface finish of 0.21 μm (R_a) was thermally oxidized (TO) at 650 °C for 6 h. After TO, some samples were polished to generate a smooth surface finish of 0.04 μm (R_a). Some were unpolished in the as-oxidized state. The effect of these two different surface finishes on the dry sliding wear behaviour was investigated. Particular attention was paid to the effect of surface finish on the formation and propagation of surface cracks and the integrity of the oxide layer during dry sliding.

2. Material and Methods

Commercially pure (CP) zirconium, grade 2, was used as the substrate material. The CP-Zr was supplied by Goofellow UK Ltd in the form of 1 mm thick sheets with the following nominal composition: 0.16 wt% O, 0.025 wt% N, 0.05 wt% C, 0.005 wt% H, 0.2 wt% Fe, 0.2 wt% Hf and Zr (rest). Before TO, the samples (20 mm x 15 mm) were ground using P1200 grade metallographic grinding paper, which produced a surface finish of 0.21 μm (R_a). The samples were then cleaned in methanol and dried in a stream of hot air.

Thermal oxidation (TO) of the samples was implemented in an air furnace at 650 °C for 6 h, which is the optimum condition determined previously [11]. The TO process conditions and the structural features of the resultant oxidized layers have been reported elsewhere [11]. The

cross-sectional view of the TO sample and the microhardness profile measured in the cross section are shown in Fig. 1. TO produced a dark and uniform oxide layer (OL) of 6.3 μm thick at the surface and a 2.8 μm thick oxygen diffusion zone (ODZ) in the subsurface. Although increasing TO time could increase OL and ODZ thicknesses, this could lead to pore formation in the oxide layer due to oxidation breakaway of zirconium [11, 28]. The hardness of the oxide layer was about 1300 $HV_{0.025}$, a typical value reported for bulk ZrO_2 [5]. The hardness decreased gradually across the ODZ to reach the substrate base level of about 200 $HV_{0.025}$.

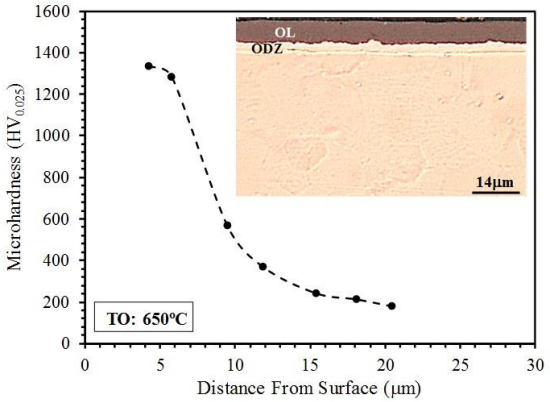

Fig. 1: Microhardness profile measured across the oxide layer (OL) and the oxygen diffusion zone (ODZ) in the cross section and microscopic image showing the cross-sectional morphology (inset) of the oxidized sample.

After TO for 6 h, the surface roughness (R_a) value was slightly increased from 0.21 μm to 0.23 μm. Some of the TO samples were polished to achieve a smoothened surface with a finish of 0.04 μm (R_a). These polished samples are designated as "TO-polished", and the TO samples in the as-oxidized state without further polishing are designated as "TO-unpolished" in this paper. Fig. 2 compares the surface roughness profiles measured from the untreated, the TO-unpolished and TO-polished samples. It can be seen that polishing considerably smoothened the TO surface and this polishing operation removed some material (0.3~0.4 μm thick) from the TO surface. This resulted in a slightly reduced oxide layer thickness.

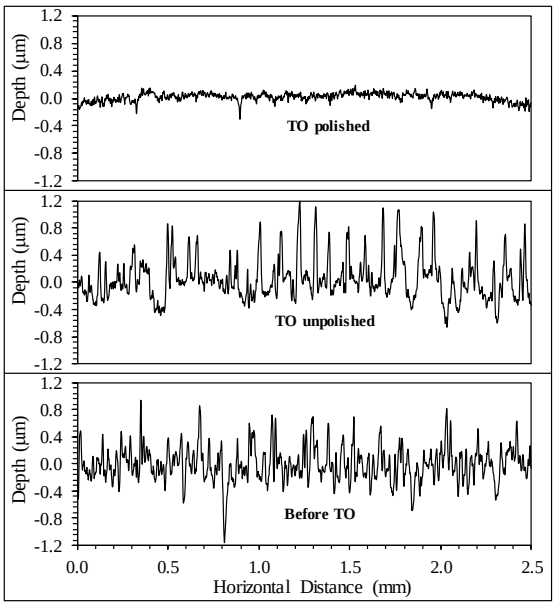

Fig. 2: Surface roughness profiles measured before TO, after TO and after polishing.

Oxidized Zr is used as bearing components in artificial implants which are subjected to tribocorrosion involving combined mechanical wear and corrosion actions [14], but it also has potential uses in other fields involving dry sliding wear [5,6]. The main focus of this work was on the dry sliding wear behaviour of the TO samples with two different surface finishes. For this purpose, tribological tests were done using the pin-on-disk configuration under dry unlubricated conditions. A 7.9 mm diameter alumina ball (Grade 25 Al_2O_3) served as the counterface slider which was kept stationary during the test. The test sample was rotating against the slider at 60 rpm for 3600 s, producing a circular wear track of 8 mm diameter. During the test, the coefficient of friction (COF) was measured continuously by the use of an integrated strain gauge and a computer data acquisition system. Two normal contact loads, 10 N and 20 N, were employed, which corresponded to initial contact pressures of about 1100 MPa and 1400 MPa, respectively, according to Hertz contact analysis based on the alumina ball contacting the untreated CP-Zr.

The wear volume was evaluated by using a stylus profilometer to measure the wear track profiles. From each profile, the cross-sectional area of the wear track was calculated and the wear volume was obtained by multiplying the cross-sectional area by the wear track circumference length. All tests were repeated twice and the average results are presented. After wear testing, an optical microscope and a scanning electron microscope (SEM) (equipped with EDX facilities for elemental composition analysis) were used to examine the worn surfaces in order to derive the wear mechanisms involved. To provide an inclined and enlarged view of the actual wear depth and the subsurface beneath the wear track, a ball crater was made on the wear track using a rotating bearing steel ball of 25.4 mm diameter. Such a ball-cratering technique has been widely used for measuring the thickness of thin coatings. It has recently been employed to aid in the examination of coating deformation beneath a wear track [29].

3. Results

Fig. 3a shows the COF curves recorded for the samples at 10 N load. Due to the dominance of plastic deformation in the untreated sample, the polished and unpolished untreated samples showed similar frictional behaviour. Thus only the COF curve for the unpolished sample is included for clarity purpose. From Fig. 3a, it can be seen that in the steady state after about 1000 s sliding, the TO-unpolished sample showed higher friction than the TO-polished sample. However, at the beginning up to 800 s, the TO-unpolished sample experienced lower friction than the TO-polished sample, which could be explained by the smaller contact area in the unpolished sample due to the initial asperity contact. It is also noted that in the steady state, the TO-unpolished sample showed higher friction than the untreated sample, while polishing after TO treatment was beneficial in lowering friction. As discussed later, under small contact loads (10 N), the OL did not suffer from any serious damage and was not worn through. Thus, the COF curves shown in Fig. 3a are characteristic of the OLs and the respective surface finish conditions.

Under high contact loads (20 N), the beneficial effect of polishing on reducing friction of the TO samples diminished, instead the TO-polished sample showed higher COF than the TO-unpolished sample during the entire sliding process (Fig. 3b). The COF of the TO-unpolished sample increased continuously during sliding, which could be related to the fact that the contact area also increased with time. The TO-polished sample initially followed the same trend, but after about 2000 s sliding, its COF started to decline, which may suggest a change in wear mechanism.

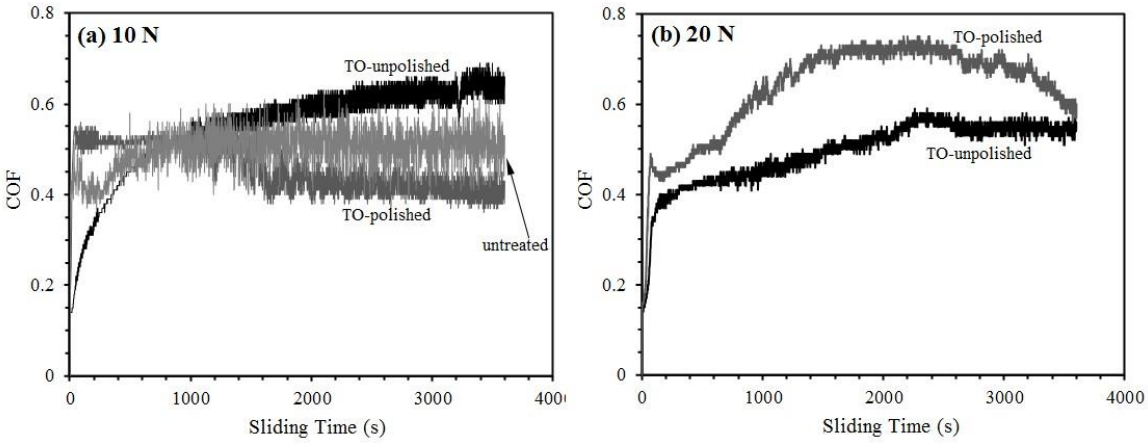

Fig. 3: Coefficient of friction (COF) curves for the tested samples recorded during dry sliding under (a) 10 N and (b) 20 N contact loads.

The measured wear volumes from the wear tracks are summarized in Fig. 4. Surface finish did not have a significant effect on wear behaviour of the untreated sample, most likely due to the dominance of plastic deformation. At the smaller load of 10 N, the wear volume of CP-Zr was reduced by up to 100 times by the thermal oxidation treatment. Polishing after TO further reduced the wear volume of the TO sample. Polishing reduced the wear volume by 137%, as compared to the corresponding TO-unpolished sample. However, as the contact load was increased to 20 N, polishing after TO had an opposite effect on wear volume of the TO sample: polishing resulted in an increase in wear volume by 41%.

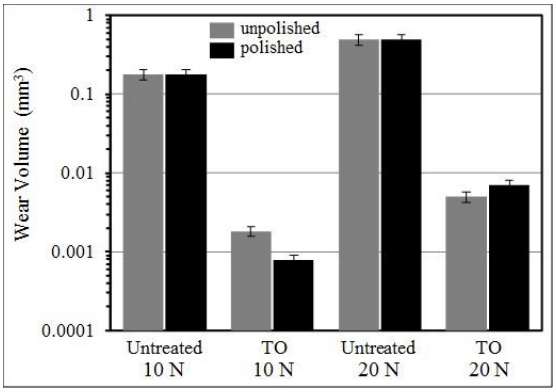

Fig. 4: Measured wear volume for the tested samples after dry sliding for 3600 s under 10 N and 20 N contact loads.

Clearly, the effect of surface finish was load dependent. At low contact loads (10 N), smoothening the TO surface was beneficial in further reducing friction and wear, while at high contact loads (20 N), a slightly rough TO surface seemed more beneficial. To have a better understanding of the wear mechanisms and material deformation behaviour involved during sliding, the worn surfaces and subsurfaces were examined microscopically, as presented in the following paragraphs.

Fig. 5 presents SEM micrographs taken from the wear tracks on the TO samples produced under 10 N contact load. After 3600 s sliding, the TO-unpolished sample suffered from mild abrasive wear as some abrasion marks, together with some original grinding marks can be seen in the wear track (Fig. 5a). No cracks were observed in the wear track on the TO-unpolished

sample. Interestingly, for the TO-polished sample, in addition to the parallel abrasion marks, many cracks, which ran across the sliding track and had a nearly semi-circular shape, were observed in the wear track (Fig. 5c and 5d). Clearly, a polished TO surface favoured the formation of cracks during dry sliding. Further examination revealed that the contact between the TO-unpolished surface and the alumina ball was at the asperity level, i.e. the sliding contact was made at the surface roughness peaks such that the roughness peaks were fragmented and fractured to generate wear debris, some of which filled the surrounding roughness valleys (Fig. 5a). Fig. 5b is a high magnification view of the real contact areas in Fig. 5a, revealing that many micro cracks were formed at the real contact areas and wear debris were generated. EDX elemental analysis revealed that the real contact areas contained a significant amount of aluminium, while in the non-contact areas, no aluminium was found (Fig. 6). This suggests that material transfer occurred from the alumina ball to the TO-unpolished surface during sliding contact. On the contrary, the contact between the TO-polished surface and the alumina ball was more uniform with the majority of the wear track area making contact with the slider (Fig. 5c). Under higher magnifications, it was found that the real contact areas on the TO-polished surface were covered with a tribofilm (Fig. 5d). EDX analysis confirmed that the real contact areas were rich in aluminium, similar to the situation shown in Fig. 6. Thus material transfer also occurred from the alumina ball to the TO-polished surface.

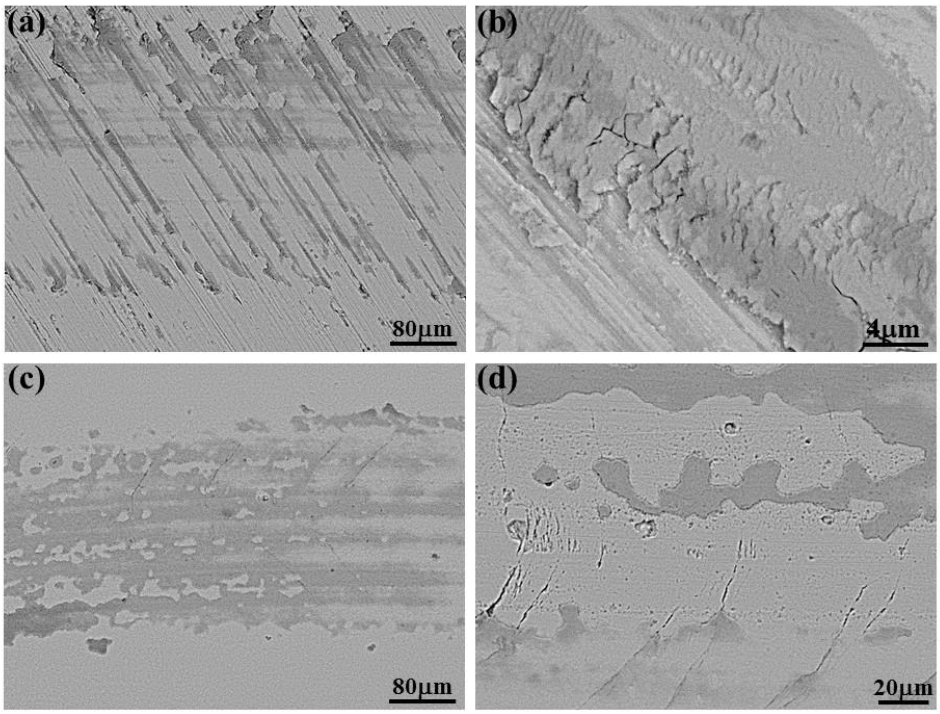

Fig. 5: SEM images showing the morphology of the wear tracks produced under 10 N contact load on the TO-unpolished sample ((a) and (b)) and on the TO-polished sample ((c) and (d)). Note the formation of cracks on the TO polished sample in (c) and (d).

Fig. 7a shows a ball crater created by rotating a 25.4 mm steel ball on the wear track produced on the TO-polished sample at 10 N load. This made the subsurface region beneath the wear track visible in an inclined view. The enlarged view of the highlighted area in Fig. 7a is given in Fig. 7b. The wear depth was just a small fraction of the OL thickness. The semi-circular cracks at the wear track surface were found to have penetrated through the OL into the ODZ and the substrate, to a depth of more than 10 microns (arrowed, Fig. 7b). No obvious plastic deformation of the oxide layer into the substrate can be observed at 10 N load, as evidenced by the maintenance of the circular contour of the interface between the OL and the ODZ in Fig.

7a. Thus it is safe to state that under the contact load of 10 N, the 6 μm thick OL, together with the underlying 3 μm thick ODZ, was effective in preventing the subsurface from plastic deformation. This may also explain why the OL could maintain its integrity with the substrate without breakdown despite the formation of many cracks which penetrated to the substrate.

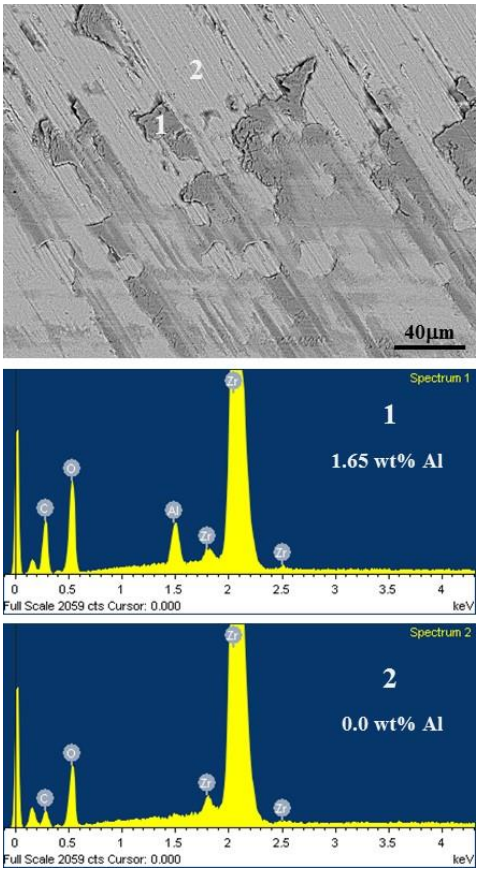

Fig. 6: SEM image and EDX elemental spot analysis in area 1 and 2 of the wear track produced under 10 N contact load on the TO-unpolished sample.

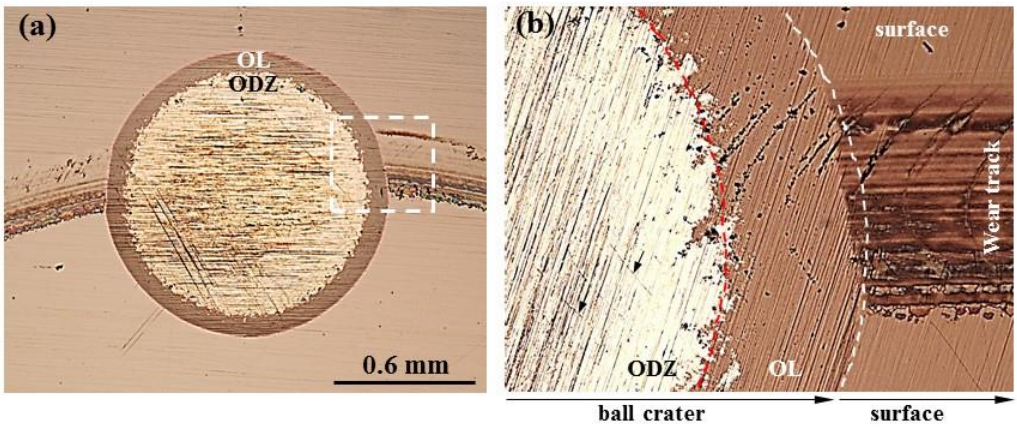

Fig. 7: (a) Microscopic image showing the ball crater made on the wear track on the TO-polished sample after dry sliding under 10 N contact load, and (b) an enlarge view of the highlighted rectangle to show crack propagation beneath the wear track. Note the circular contour of the interface between the OL and ODZ in (a) and the penetration of cracks to the substrate (arrowed) in (b).

However, at a higher contact load (20 N), the situation became quite different. Fig. 8 shows the wear tracks produced at 20 N on the TO-unpolished and TO-polished samples. The original grinding marks, together with some cracks, can be visible in the wear track on the TO-unpolished sample (Fig. 8a). Cracking and failure of the OL were much more severe on the TO-polished sample (Fig. 8b). The OL on the TO-polished sample suffered from local breakdown and severe cracking with densely populated semi-circular cracks in the wear track (Fig. 8b). A comparison with the corresponding unpolished sample confirmed again that polishing after TO indeed favoured crack formation during dry sliding. The ball crater created on the wear track on the TO-polished sample (Fig. 9a) revealed that the OL was deformed or pushed into the substrate under the 20 N load. The surface cracks also penetrated through the OL into the ODZ and the substrate (Fig. 9b). Local failure of the OL can be seen in the wear track on the TO-polished sample. SEM examination (Fig. 10) showed that the cracks on the TO-polished specimen were filled with wear debris. EDX analysis, shown in Fig. 10, revealed that there was much more aluminium in the cracks filled with wear particles than in the real contact areas outside the cracks. This demonstrates that wear of the alumina ball contributed to wear debris formation in the tribosystem.

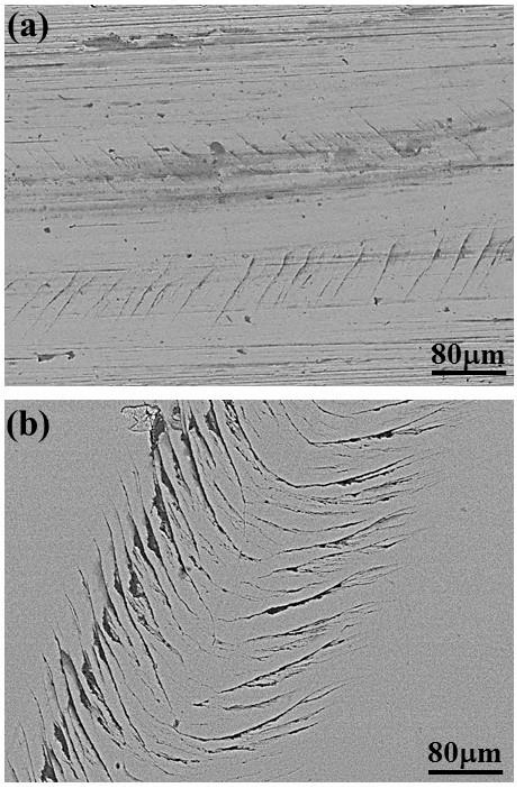

Fig. 8: SEM images showing the wear tracks produced on the (a) unpolished and (b) polished TO sample under 20 N contact load.

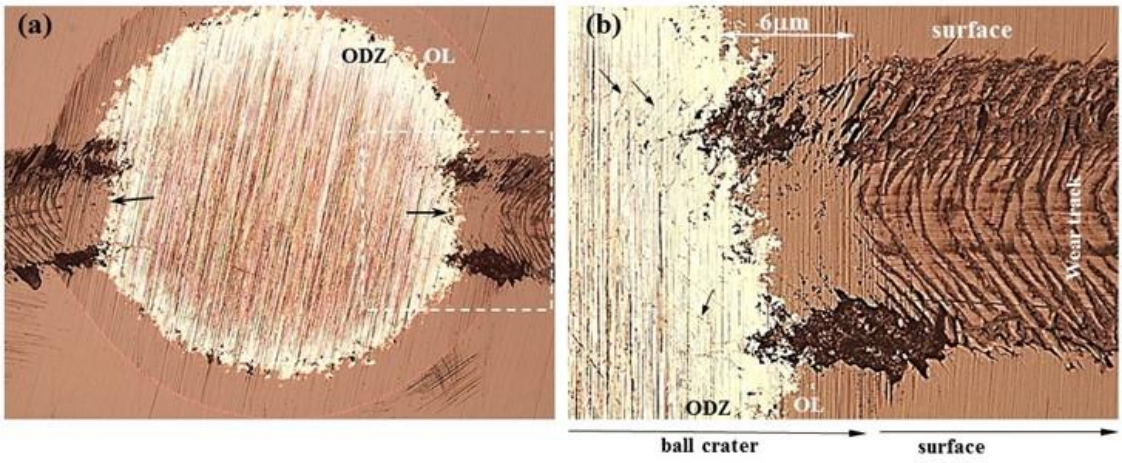

Fig. 9: (a) Microscopic image showing the ball crater made on the wear track on the TO-polished sample after dry sliding under 20 N contact load, and (b) an enlarge view of the highlighted rectangle to show crack propagation beneath the wear track. Note the deformation of the OL into the substrate in (a) (arrowed) and propagation of cracks to the substrate (arrowed) in (b).

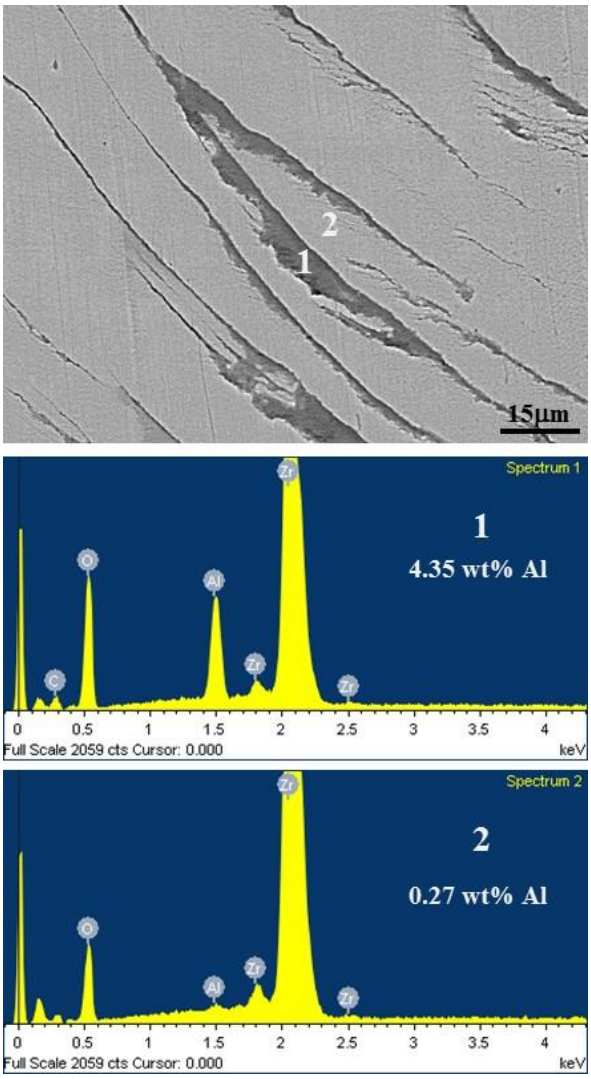

Fig. 10: SEM image and EDX elemental spot analysis of area 1 and 2 of the wear track produced under 20 N contact load on the TO-polished sample.

To gain a further insight into the contact behaviour and the development of cracks with sliding time, a series of experiments were conducted involving sliding for various times, followed by microscopic examination of the wear track and the wear scar on the counterface. Fig. 11 compares the wear tracks on the TO-polished sample after sliding at 10 N and 20 N for various times. At 10 N, the contact between the TO-polished surface and the alumina ball was confined to a narrow width during the first 300 s sliding. No cracks were observed at this stage (Fig. 11a). As sliding proceeded, the wear track width and the wear scar size on the counterface (Al_2O_3 ball) were increased. After sliding for1800 s at 10 N, semi-circular cracks started to appear (Fig. 11b). With continuous sliding to 3600 s, semi-circular cracks were fully developed on the polished sample (Fig. 5c). The development of cracks on the polished sample was load dependent. Under the higher load of 20 N, semi-circular cracks were developed after sliding for just 300 s (Fig. 11c). With continuous sliding to 900 s, the cracks were further developed with new cracks formation within the widened wear track (Fig. 11d). After sliding for 3600 s, densely populated cracks were developed, leading to the onset of OL breakdown (Fig. 9b).

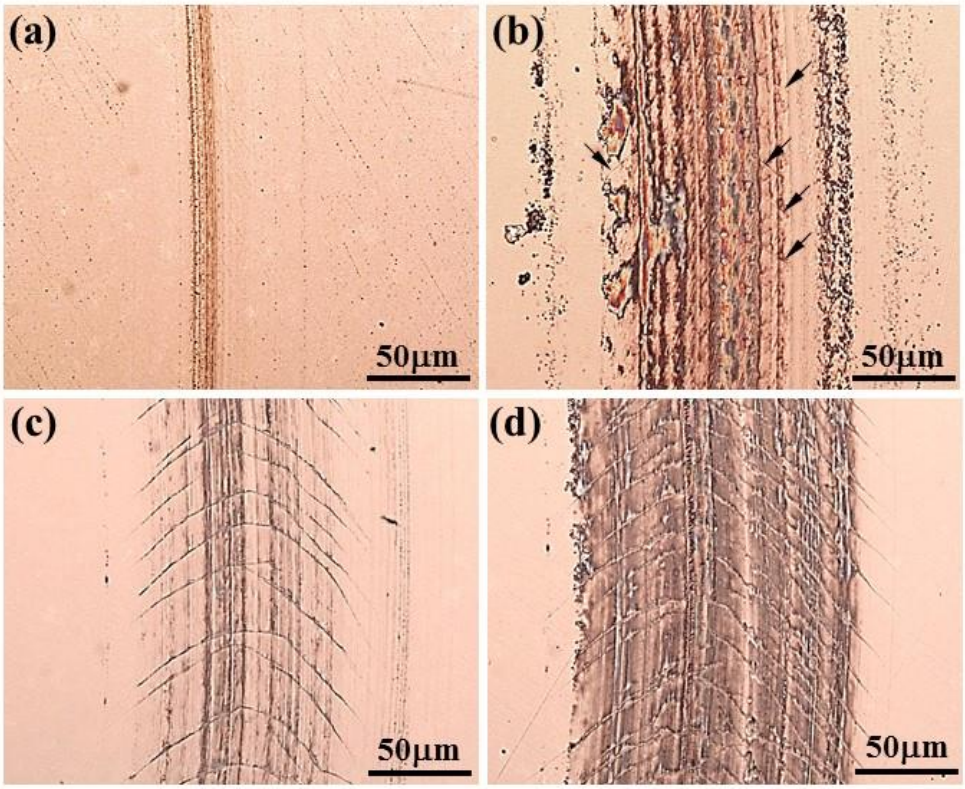

Fig. 11: Microscopic images showing the morphology of the wear tracks after dry sliding testing the TO-polished sample at 10 N for (a) 300 s and (b) 1800 s, and at 20 N for (c) 300 s and (d) 900 s. Note the formation of semi-circular cracks after sliding for 1800 s in (b) (arrowed).

In Fig. 12, the measured mean diameter of the wear scar on the counterface is plotted against sliding time at 10 N. The wear scar was larger when sliding against the TO-unpolished surface. Thus, as compared to the TO-polished surface, the TO-unpolished surface caused more wear of the counterface alumina ball, which is expected from the general principle of tribology of rough surfaces [20-24].

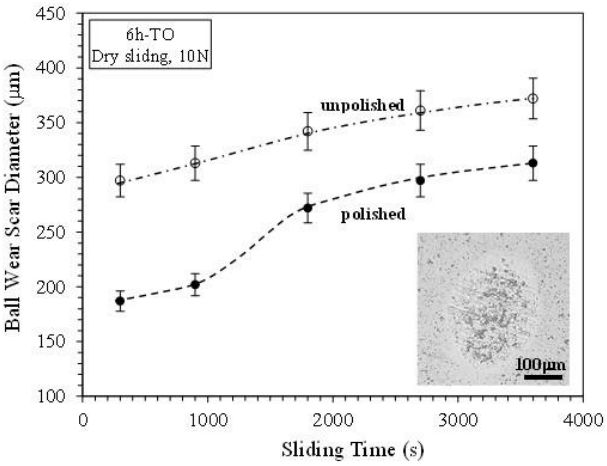

Fig. 12: Mean diameter of the wear scar on the alumina ball counterface as a function of sliding time on the TO-polished and unpolished samples.

4. Discussion

The experimental results demonstrated that surface finish affected the tribological behaviour of thermally oxidized CP-Zr in several aspects, including COF, wear volume, crack formation and breakdown of the OL. At relatively small contact loads (e.g. 10 N), smoothening the TO surface by polishing was beneficial in reducing friction (Fig. 3a) and wear volume (Fig. 4). This agrees with general observations made by other investigators for both bulk and coating materials that a rougher surface results in higher friction and higher wear rates of both the test specimen and the counterface [24,25,27]. The higher friction and wear rates resulting from rough surfaces have several origins, including the ploughing action of the surface peaks, the deformation and fracture of the asperities, the change in real contact areas, the filling of the surface roughness valleys with wear debris and the mechanical interlocking provided by the asperities. It is also generally observed that after a certain period of sliding, the surface asperities become gradually flattened and the original surface finish is destroyed, thus the initial surface finish effect on friction and wear will diminish [23].

The most striking observation made in this work is that smoothening the surface by polishing after TO favoured the formation of cracks running across the wear tracks (Fig. 5 and Fig. 8). Although at 10 N contact load, the hardened surface was effective in preventing plastic deformation in the substrate (Fig. 7a), many semi-circular cracks were developed in the wear track on the TO-polished sample, but no such cracks were found on the corresponding unpolished sample (Fig. 5). There seemed an incubation time for the formation of semi-circular cracks on the TO-polished sample, as shown in Fig. 11. Such an incubation time was load dependent: it took about 1800 s for the cracks to form at 10 N, while at 20 N, cracks formed at the very early stage of sliding (300 s). These cracks on the TO-polished sample propagated through the surface layers down to the substrate (Fig. 7 and Fig. 9). The fact that the OL did not detach or flake from the substrate indicates that the crack length was not sufficient to cause final fracture of the OL under 10 N load. According to the principle of fracture mechanics, a material fractures when a critical crack length is reached. Such a critical crack length decreases with increasing stress level. Under the present contact condition at 10 N load, the contact stress level and the crack prorogation depth were not sufficient to cause OL breakdown. Increasing the contact load to 20 N was sufficient to cause the fracture and even the local breakdown of the OL (Fig. 8b and Fig. 9b). The existence of an incubation time for the formation of cracks (Fig. 11) suggests that the fracture of the OL was a fatigue process. Thus, it can be predicted

that with prolonged sliding, the OL would breakdown at 10 N load once the cracks propagate to reach critical lengths.

In the wear tracks on the TO-unpolished sample, semi-circular cracks were not observed at 10 N and were only observed at 20 N, but to a lesser extent than those on the TO-polished sample. The beneficial effect of surface roughness in delaying semi-circular crack formation and propagation can be explained as follows. Under the present testing conditions, the contact between the TO-unpolished surface and the smooth alumina ball was at the asperity level (Fig. 5). The hard ZrO_2 asperities not only had a ploughing action on the alumina ball to result in a large wear scar on the ball (Fig. 12), but also suffered from extremely high contact pressures, as predicted by the contact models developed for rough surfaces [23,30,31]. Thus the contact stresses were concentrated at the highest asperities and the stresses in the non-contacting areas and in the bulk of the OL must be much reduced. The high stresses at the asperities resulted in the flattening of the contacting asperities through fragmentation and fracture. Although semi-circular cracks were not observed at 10 N load, many micro cracks were found at the real contact areas, which led to wear debris formation through fracture (Fig. 5b). Thus the micro cracks at the contacting asperities did not have the opportunity to develop into larger cracks in the bulk of the OL at 10 N load. With increasing sliding time, more asperities were brought into contact and the ball wear scar size increased (Fig. 12). The increased apparent and real contact areas helped to reduce contact stresses at the asperities. Semi-circular cracks were only able to form in the smoothened areas at 20 N (Fig. 8a), where asperity deformation and fracture became less dominant.

5. Conclusions

The dry sliding wear behaviour of TO-unpolished and TO-polished CP-Zr samples were investigated. The main findings are summarized as follows:

(1) Smoothening the oxidized surface by polishing is beneficial in reducing friction and wear volume of the TO sample if the contact load is relatively small (10 N).

(2) Under high contact loads (20 N), smoothening the oxidized surface deteriorates the wear resistance of the TO sample and accelerates the breakdown of the oxide layer.

(3) Smoothening the oxidized surface by polishing favours the formation of large semi-circular cracks in the wear tracks during dry sliding under both contact loads.

(4) The semi-circular cracks developed at the TO-polished surface propagate through the surface layers to reach the substrate. This leads to the local breakdown of the oxide layer after sliding for a certain period of time under sufficiently large contact loads (e.g. 20 N).

(5) A slightly rough TO surface (unpolished) is beneficial in reducing the tendency of the oxide layer towards cracking during dry sliding, owing to the dominance of asperity contacts which lead to micro crack formation at the real contact areas and fracture of the contacting asperities.

Acknowledgement:

The Saudi Cultural Bureau in London is acknowledged by one of the authors (AA) for providing a PhD scholarship to facilitate this research.

References

[1] IAEA. Waterside corrosion of zirconium alloys in nuclear power plants [M]. VIENNA, 1998, IAEA-TECDOC-996, ISSN 1011-4289.

[2] HUNTER G, DICKINSON J, HERB B, GRAHAM R. Creation of oxidized zirconium orthopaedic implants. L. D Zardiackas, M.J. Kraay, H.L. Freese (Eds.), Titanium, Niobium, Zirconium, and Tantalum for Medical and Surgical Applications [M]. ASTM STP 1471, American Society for Testing and Materials, West Conshohocken, PA (2006), pp. 16–29.

[3] CHEVALIER J. What future for zirconia as a biomaterial? [J]. Biomaterials, 2006, 27: 535–543.

[4] WEBSTER R T. Zirconium for chemical processing applications [J]. Metals Progress, 1978, 113 (2): 62-64.

[5] HAYGARTH J C, FENWICK L J. Improved wear resistance of zirconium by enhanced oxide films [J]. Thin Solid Films, 1984, 118: 351-362.

[6] JI R, LI X Y, DONG H. Ceramic conversion treatment of zirconium alloys to combat wear [J]. Surface Engineering, 2010, 26: 30-36.

[7] HUNTER G, ASGIAN C M, HINES G I. Methods of surface hardening zirconium alloys and resulting products [J]. United States Patent, US 6447550 [P], 2002.

[8] PAWAR V, WEAVER C, JANI S. Physical characterization of a new composition of oxidized zirconium-2.5 wt% niobium produced using a two step process for biomedical applications [J]. Applied Surface Science, 2011, 257: 6118-6124.

[9] CHENG Ying-liang, WU Fan. Plasma electrolytic oxidation of zircaloy-4 alloy with DC regime and properties of coatings [J]. Transactions of Nonferrous Metals Society of China, 2012, 22: 1638-1646.

[10] WANG L, HU X, NIE X. Deposition and properties of zirconia coatings on a zirconium alloy produced by pulsed DC plasma electrolytic oxidation [J]. Surface & Coatings Technology, 2013, 221: 150–157.

[11] ALANSARI A, SUN Y. Effect of oxidation time on the tribological behavior of thermally oxidized commercially pure zirconium under dry sliding conditions [J]. Surface & Coatings Technology, 2017, 309: 195-202.

[12] PATEL A M, SPECTOR M. Tribological evaluation of oxidized zirconium using an articular cartilage counterface: a novel material for potential use in hemiarthroplasty [J]. Biomaterials, 1997, 18: 441-447.

[13] GOOD V, WIDDING K, HUNTER G, HEUER D. Oxidized zirconium: a potentially longer lasting hip implant [J]. Materials Design, 2005, 26: 618-622.

[14] GALETZ M C, FLEISCHMANN E W, KONRAD C H, SCHUETZ A, GLATZEL U. Abrasion resistance of oxidized zirconium in comparison with CoCrMo and titanium nitride coatings for artificial knee joints [J]. Journal of Biomedical Materials Research Part B, 2010, 93: 244–251.

[15] DESJARDINS J D, BURNIKEL B, LABERGE M. UHMWPE wear against oxidized zirconium and CoCr femoral knee components during force-controlled simulation [J]. Wear, 2008, 264: 245-256.

[16] EZZET K A, HERMIDA J C, STEKLOV N, D'LIMA D D. Wear of polyethylene against zirconium femoral components [J]. The Journal of Arthroplasty, 2012, 27:116-121.

[17] INNOCENTI M, MATASSI F, CARULLI C, NISTRI L, CIVININI R. Oxidized zirconium femoral component for TKA: a follow-up note of a previous report at a minimum 10 years [J]. The Knee, 2014, 21: 858-861.

[18] SVAHN F, KASSMAN-RUDOLPHI A, WALLEN E. The influence of surface roughness on friction and wear of machine element coatings [J]. Wear, 2003, 254: 1092-1098.
[19] HANIEF M, WANI M F. Effect of surface roughness on wear rate during running-in of En31-steel: model and experimental validation [J]. Materials Letter, 2016, 176: 91-93.
[20] BAYER R G, SIRICO J L. The influence of surface roughness on wear [J]. Wear, 1975, 35: 251-260.
[21] FEDERICI M, MENAPACE C, MOSCATELLI A, GIALANELLA S. Effect of roughness on the wear behaviour of HVOF coatings dry sliding against a friction material [J]. Wear, 2016, 368-369: 316-334.
[22] RAHAMAN M L, ZHANG L, LIU Mei, LIU W. Surface roughness effect on the friction and wear of bulk metallic glasses [J]. Wear, 2015, 332-333: 1231-1237.
[23] JIANG J, ARNELL R D. The effect of substrate surface roughness on the wear of DLC coatings [J]. Wear, 2000, 239: 1-9.
[24] TAKADOUM J, BENNANI H H. Influence of substrate roughness and coating thickness on adhesion, friction and wear of TiN films [J]. Surface & Coatings Technology, 1997, 96: 272-282.
[25] KUBIAK K J, LISKIEWICZ T W, MATHIA T G. Surface morphology in engineering applications: influence of roughness on sliding and wear in dry fretting [J]. Tribology International, 2011, 44: 1427-1432.
[26] LEE S C, HO W Y, LAI F D, Effect of substrate surface roughness on the characteristics of CrN hard film, Mater [J]. Chemical Physics. 1996, 43: 266-273.
[27] BULL S J, CHALKER P R, JOHNSTON C, MOORE V. The effect of roughness on the friction and wear of diamond thin films [J]. Surface & Coatings Technology, 1994, 68-69: 603-610.
[28] PLOC R A. An electron microscope study of breakaway oxidation of zirconium at 623 K [J]. Journal of Nuclear Materials, 1980, 91: 322-328.
[29] SUN Y, DEARNLEY P A, MALLIA B. Response of duplex Cr(N)/S and Cr(C)/S coatings on 316L stainless steel to tribocorrosion in 0.89 % NaCl solution under plastic contact conditions [J]. Journal of Biomedical Materials Research Part B, 2017, 105: 1503-1513.
[30] MAO K, SUN Y, BELL T. A numerical model for dry sliding contact of layered elastic bodies with rough surfaces [J]. STLE Tribology Transactions, 1996, 39(2): 416-424.
[31] MAO K, SUN Y, BLOYCE A, DONG H. Surface coating effects on contact stress and wear: an approach of surface engineering design and modelling [J]. Surface Engineering, 2010, 26: 142-148.

表面光洁度对氧化处理工业纯锆的干磨损性能的影响

A. Alansari, Y. Sun

School of Engineering and Sustainable Development, Faculty of Technology, De Montfort University, Leicester, UK

摘要：本文的目的为研究在干磨条件下表面光洁度对氧化处理工业纯锆(CP-Zr)的磨擦磨损性能的影响。CP-Zr 试样经表面打磨后(R_a=0.21 μm)，在 650°C 温度下氧化 6 个小时。氧化后，有的试样经过抛光而取得镜面光洁度(R_a=0.04 μm)。采用单向滑动试验方法对抛光和未抛光的氧化试样进行了比较测试。结果表明，表面抛光对氧化 CP-Zr **的干磨擦**磨损**性能有**较大的影响，包括磨擦系数，磨损量，裂文形成和氧化层破裂。表面抛光加快了在干磨擦过程中半圆形裂纹的形成和氧化层的破裂。**在高接触**应力下, 稍为粗造点的**氧化表面有利于**减缓裂文的形成和提高耐磨性。本文对磨损机理，裂文形成，扩展和断裂进行了探讨。

关键词：锆，热氧化，氧化锆，表面光洁，磨擦，磨损